# Deuterium NMR of polymer dispersed liquid crystals

A. Golemme, S. Žumer,* and J. W. Doane
*Department of Physics, Kent State University, Kent, Ohio 44242-0001*

M. E. Neubert
*Liquid Crystal Institute, Kent State University, Kent, Ohio 44242-0001*
(Received 27 July 1987)

Submicrometer-size droplets of monomeric liquid crystals dispersed in a solid polymer matrix are studied by deuterium NMR. Phase-separation processes are used to achieve droplets of a size comparable and less than the magnetic coherence length $\xi \sim 0.5$ $\mu$m, of the NMR magnetic field, 4.7 T. Selectively deuterated (4'-pentoxy- and 4'-methoxy-) 4-cyanobiphenyl compounds (5OCB-$d_2$) and (1OCB-$d_3$) deuterated in the $\alpha$ and methyl positions, respectively, provide for two different NMR measurement time scales to examine effects of the self-diffusion of the molecules confined to droplets. It is found that the line shape of the spectra depends on several factors which include self-diffusion, size, shape of the droplets, and type of anchoring on the droplet walls. Theoretical director configurations calculated for spherical and nonspherical droplets in the presence of an external field were used to simulate NMR spectra in the presence of self-diffusion. Effects due to external fields present during sample preparation are discussed.

## I. INTRODUCTION

Recent advances in optical and electro-optical devices technology have been made possible using materials consisting of submicrometer-size nematic droplets embedded in a polymer matrix.[1,2] The operation of these devices depends on the type of nematic director configuration[3] inside the droplet and its response to an applied field. Relatively large nematic droplets ($d \gg 1$ $\mu$m) formed in a liquid have been studied using optical microscopy,[4,5] but there is practically nothing known about submicrometer-size droplets. In addition to light scattering,[6] deuterium nuclear magnetic resonance can be used to directly study some features of nematic materials confined to a submicrometer-size droplet.

The surface competes with the field of the NMR magnet in aligning the directors inside a droplet. The range of the surface influence is estimated by the magnetic coherence length $\xi$ which when assuming infinitely strong anchoring is given by[7]

$$\xi = \left[ \frac{\mu_0 K}{\Delta\chi} \right]^{1/2} \frac{1}{B} , \tag{1}$$

where $K$ can be either $K_1$ or $K_2$ or $K_3$ or somewhere in between depending on the geometry and $\Delta\chi$ stands for $|\chi_{\parallel} - \chi_{\perp}|$. In the materials studied, it is possible to achieve droplets of predetermined size from 0.1 to 10 $\mu$m in diameter. The NMR field of 4.7 T provides a coherence length $\xi \simeq 0.5$ $\mu$m, therefore requiring droplets with a diameter $d < 1$ $\mu$m in order to prevent significant distortion of the director configuration by the magnetic field. In Sec. II we discuss some director configurations in a droplet. Section III is devoted to deuterium nuclear magnetic resonance (DMR) line-shape derivation in which the effects due to the high surface-to-volume ratio and restricted translational diffusion in the nematic phase are taken into account.

It is worthwhile to mention some other effects characteristic of droplets which we are not going to discuss in detail. Collective modes have an upper bound to a possible wavelength and they are also affected by the director structure in the droplet. In very small droplets, bend deformations can induce biaxiality. Defects and strong surface anchoring introduce some positional variations in the degree of the orientational order over the volume of the droplet.[8]

Section IV describes two methods used to prepare our materials: polymerization-induced phase separation (PIPS), in which phase separation of the liquid crystal into droplets is achieved during the polymerization process of an initially homogeneous solution of liquid crystals and monomers and thermally induced phase separation (TIPS), in which a homogeneous solution of liquid crystals and a thermoplastic is cooled from a temperature where the components are completely miscible to a temperature where they are only partially miscible. Sec. V is devoted to the presentation of experimental results and the comparison with line-shape simulations. The use of DMR to monitor the effect of droplet distortions introduced by a mechanical stress or by strong external fields applied during the formation of the droplets is described as well. The influence of droplet radii and of the strength of the quadrupolar coupling spectral width on the line shape is also discussed.

## II. DIRECTOR CONFIGURATION IN NEMATIC DROPLETS

The expected director configuration of a nematic liquid crystal in a spherical droplet has been calculated and microscopically verified in large droplets by several

 

workers.[3–5,9–11] The structure of nematic droplets has been obtained by minimization of the elastic free energy for different types of molecular anchoring on the droplet surface in the presence of an external field.[3] Other authors reported the observation of twisted configurations[9] and the consequent possibility of different kinds of phase transitions either with or without the presence of an external field.[10] Recently the toroidal (axial) configuration has been experimentally observed[11] using liquid crystals with a low bend-to-splay ratio. In this case the nematic director is tangential at the interface and always normal to a central line disclination corresponding to a diameter of the sphere. Using large droplets, where elastic energy constraints become less severe, the dynamics of the transformation or of the creation and annihilation of topological defects has been studied[5] both theoretically and experimentally.

In this paper we will deal with director configurations calculated in the approximation of a single elastic constant $K_1=K_2=K_3=K$. In this case the external field and the elastic contributions to the free energy of a nematic droplet can be written as[6]

$$F=\tfrac{1}{2}\int\left[K[(\nabla\cdot\mathbf{n})^2+(\nabla\times\mathbf{n})^2]-\frac{\Delta\chi}{\mu_0}(\mathbf{B}\cdot\mathbf{n})^2\right]dV\ . \qquad (2)$$

Here, as well, we neglect surface-induced effects on the value and anisotropy of the order parameter[6,12] and assume strong molecular anchoring on the droplet surface. The minimization of the free energy $F$ [Eq. (2)] results in a partial differential equation[6] which is solved using the nonlinear over-relaxation method.[13]

Figure 1 shows several director configurations, calculated for diametral sections of spherical and nonspherical droplets. Since we limit our treatment to configurations with cylindrical symmetry, three-dimensional (3D) patterns can be obtained by rotation of these sections around the symmetry axis.

In the case of parallel molecular anchoring on the surface and single-elastic-constant approximation, the preferred configuration, but not the only possible one, is bipolar with two surface-point defects aligned along the external field [see Figs. 1(a) and 1(c)]. The strength of the applied field does not change the general features of the structure but only the degree of the director orientation in the droplet.

For normal anchoring the director configuration strongly depends on the strength of the applied field. For $R/\xi<4$, where $R$ is the radius of a spherical droplet, the lowest free energy corresponds to the "star" configuration, with a point defect in the center [see Fig. 1(b)]. At a value of $R/\xi\approx 4$, there is a phase transition to a configuration with an equatorial line disclination characteristic for $R/\xi>4$ [see Fig. 1(d)]. Figures 1(e) and 1(f) show structures in the case of prolate ellipsoids which can be experimentally achieved by a uniaxial mechanical stress.

In the case of large droplets, $R\gtrsim 1$ $\mu$m, the director configuration can be directly monitored using an optical microscope with crossed polarizers. Very distinctive patterns can be observed corresponding to different

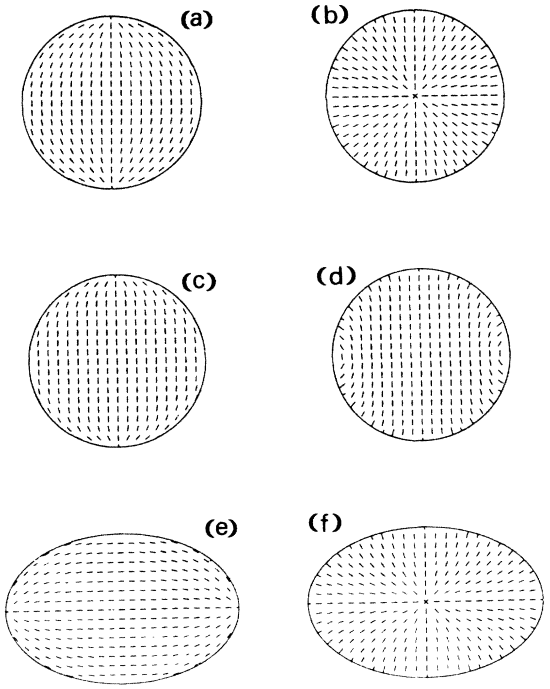


FIG. 1. Nematic director configuration for tangential [(a), (c), (e)] and normal [(b), (d), (f)] surface anchoring in spherical and prolate ellipsoidal droplets. The sections are diametral planes. Configurations (c) and (d) are obtained by applying a "strong" field in a direction parallel to the droplet director.

configurations and, ultimately, to different surface anchorings of the liquid crystal.[4] Figure 2 shows nematic droplets with tangential surface anchoring with an average radius of approximately 4 $\mu$m dispersed in a thermoplastic polymer as observed between crossed polarizers.

## III. DEUTERIUM NMR LINE SHAPES

The molecular orientational order in nematic droplets strongly influences the DMR line shape. Because of the positional dependence of the molecular orientation, molecular self-diffusion can induce additional motional averaging. Considering typical values for the translational diffusion coefficient, $D\simeq 10^{-6}$ cm$^2$/sec, and for a droplet diameter $R\simeq 1$ $\mu$m, we find from the relation $6Dt=d^2$ that spectra with splittings in the 1.0 kHz range will be motionally averaged while spectra in the 100 kHz range will be little affected by diffusion. Let us first neglect translational motions and in a frame determined by the external field $\mathbf{B}$ write the angular quadrupolar frequencies for a nucleus with spin $I=1$ at the position $\mathbf{r}$ as

$$\omega_q(\mathbf{r})=\pm\pi\delta\nu(\mathbf{r})\tfrac{1}{2}\{3\cos^2\theta(\mathbf{r})-1+\eta(\mathbf{r})\sin^2\theta(\mathbf{r})\cos[2\phi(\mathbf{r})]\}\ , \qquad (3)$$

where $\delta\nu(\mathbf{r})$ is the local quadrupolar splitting of the bulk nematic. The asymmetry parameter $\eta(\mathbf{r})$ can be different from zero in the droplet, because the averaging motions (orientational fluctuations) lose their symmetry

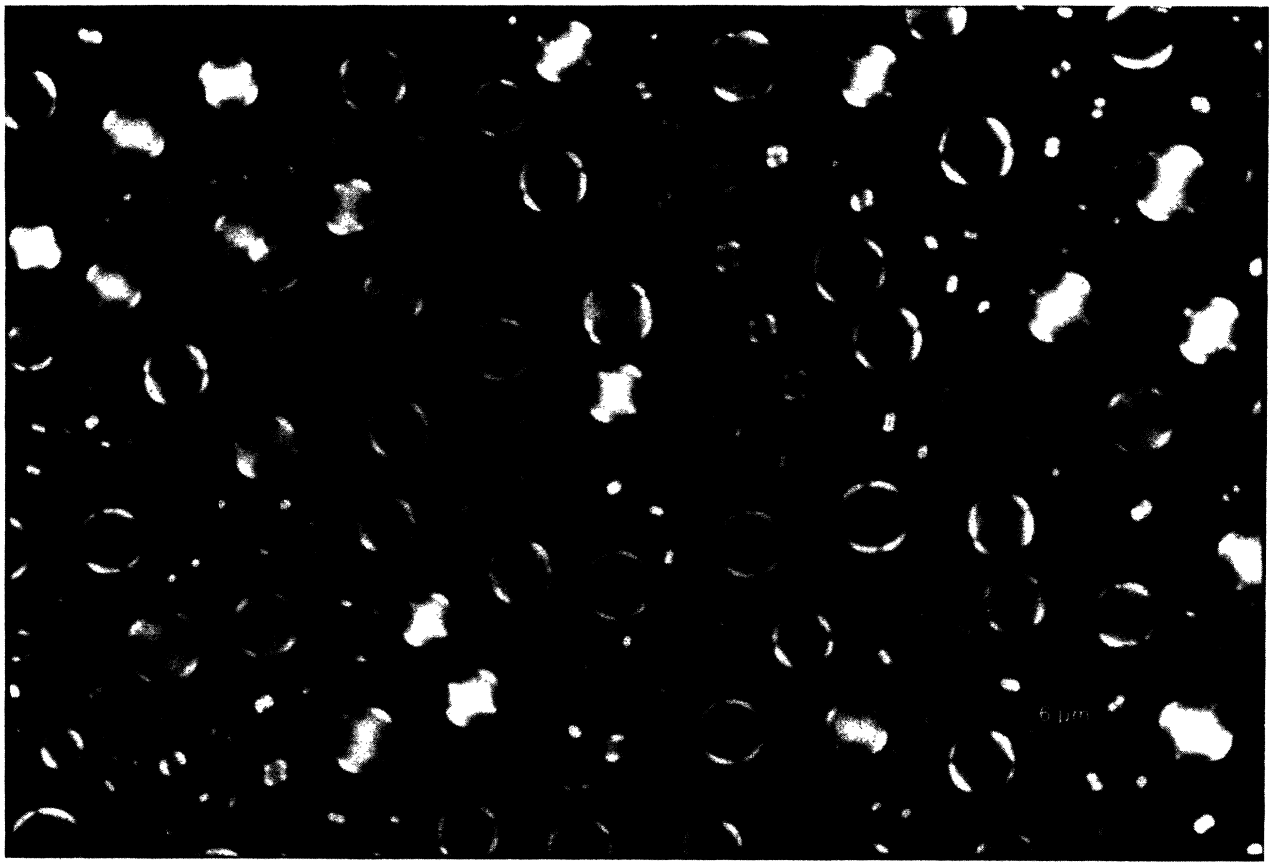

FIG. 2. Optical microscope picture of droplets of British Drug House E7 dispersed in an epoxy resin obtained by mixing equal amounts of Epon 828 and *t*-butylamine. The sample is positioned between crossed polarizers.

due to the confinement. The polar angles $\theta(\mathbf{r})$ and $\phi(\mathbf{r})$ express the orientation of **B** in the principal axis frame of the local electric field gradient (EFG) tensor averaged over fast orientational fluctuations.

The effect of motional averaging due to the translational diffusion can be taken into account using the semiclassical approach in which the molecular motion is introduced with a time-dependent Hamiltonian.[14] The line shape is given by

$$I(\omega)=\int e^{-i\omega t}G(t)dt \ , \tag{4}$$

where

$$G(t)=e^{i\omega_Z t}G_q(t) \tag{5}$$

and

$$G_q(t)=\left\langle \exp\left[ i\int_0^t \omega_q(\mathbf{r}(t')dt' \right] \right\rangle . \tag{6}$$

Here $\omega_Z$ is the Zeeman frequency, $\omega_q(\mathbf{r}(t'))$ is the instantaneous value of the quadrupolar frequency shift corresponding to the position $\mathbf{r}(t')$ and $\langle\ \rangle$ stands for the ensemble average. This treatment does not include the effect of lifetime broadening, which can be introduced by convoluting $I(\omega)$ with a Lorentian curve whose width is approximately $1/T_1$.

The calculation of the $G_q(t)$ defined by Eq. (6) requires adequate ways to describe the position of a molecule, $\mathbf{r}(t)$, and to perform averages over all possible initial states and over all possible molecular "paths." Comparing the molecular size, $\sim 10$ Å, and the droplet diameter, $\sim 0.5$ $\mu$m, one can see that the average molecular orientation does not change on the molecular scale in jumping from one site to the next. Therefore, the details of the diffusion process do not affect motional averaging and we are going to use a simple random jump diffusion model. In this approach the time is divided into short intervals of length $\tau$ so that the frequency $\omega_q$ can be represented by a step function.

If we introduce a probability $W(i,i+1)$ for the "transition" from the position $i$ to the position $i+1$ and a probability $P(1)$ for the initial "state," then we can write the relaxation function as a $p$-fold integral,

$$G_q(t)=\int \cdots \int P(1)e^{i\omega_q(\mathbf{r}_1)\tau}W(1,2)e^{i\omega_q(\mathbf{r}_2)\tau}W(2,3)\cdots W(p-1,p)e^{i\omega_q(\mathbf{r}_p)\tau}d^3r_1\cdots d^3r_p \ . \tag{7}$$

Increasing the number of dimensions $p$, the probabilities $W(i-1,i)$ are more and more restricted to small parts of the

whole volume.

In the following we discuss line shapes of spherical and ellipsoidal droplets with at least cylindrically symmetric nematic structures. The axis of cylindrical symmetry will be called droplet director **N**. At each position $\mathbf{r}=(r,\theta,\phi)$ in the droplet we introduce $\theta_n(\mathbf{r})$ and $\phi_n(\mathbf{r})$ (see Fig. 3) as orientation angles of the local director (as well as the $z$ principal axis of the EFG) in the droplet frame. If local ordering is biaxial, an additional angle, $\phi_b(\mathbf{r})$, defining the direction of the $\mathbf{n}_b$, the second principal axis of the EFG, must be introduced (see Fig. 3). In addition, we must introduce the angles $\theta_N$, between droplet director **N** and magnetic field **B**, and $\theta$, between the director **n** and **B**.

Introducing angles defined above to Eq. (3) we have

$$\omega_q=\pm\pi\delta\nu\tfrac{1}{2}\{\eta-1+(3-\eta)(\cos\theta_n\cos\theta_N+\sin\theta_n\sin\theta_N\cos\phi_n)^2 -2\eta[\sin\phi_b(\cos\theta_N\sin\theta_n-\sin\theta_N\cos\theta_n\cos\phi_n)-\cos\phi_b\sin\theta_N\sin\phi_n]^2\}\ . \tag{8}$$

Diffusion will be described as a random-jump process on a square lattice, where a molecule is allowed to jump only to one of the six nearest neighboring sites. On the droplet surface we assume diffusion reflection.

In an isotropic environment the mean-square displacement is given by $\langle\Delta r^2\rangle=\langle\Delta x^2\rangle+\langle\Delta y^2\rangle+\langle\Delta z^2\rangle=6Dt$ but in an anisotropic medium, if we are in the eigenframe $(x_0,y_0,z_0)$ of the diffusion tensor $\underline{\mathbf{D}}$ we have

$$\langle\Delta x_0^2\rangle=\langle\Delta y_0^2\rangle=2D_\perp t \quad\text{and}\quad \langle\Delta z_0^2\rangle=2D_\parallel t \tag{9}$$

with $D_\perp$ and $D_\parallel$ as eigenvalues of $\underline{\mathbf{D}}$, where the underline is used to denote a tensor. In an inhomogeneous medium such as our droplets, Eq. (9) is valid only for displacements confined to a small volume where the director alignment is quasiuniform. We chose our lattice in the droplet frame with the $z$ axis parallel to **N** and we transform $\Delta\mathbf{r}_0$ from the eigenframe of $\underline{\mathbf{D}}$ to the droplet frame,

$$\Delta\mathbf{r}=\begin{bmatrix}\cos\phi_n(\Delta x_0\cos\theta_n+\Delta z_0\sin\theta_n)+\Delta y_0\sin\phi_n\\ -\sin\phi_n(\Delta x_0\cos\theta_n+\Delta z_0\sin\theta_n)+\Delta y_0\cos\phi_n\\ -\Delta x_0\sin\theta_n+\Delta z_0\cos\theta_n\end{bmatrix}\ . \tag{10}$$

Performing the averaging and using Eq. (9) follows,

$$\langle\Delta x^2\rangle=2D_\perp t(\cos^2\phi_n\cos^2\theta_n+\sin^2\phi_n)+2D_\parallel t\sin^2\theta_n\cos^2\phi_n\ , \tag{11a}$$

$$\langle\Delta y^2\rangle=2D_\perp t(\sin^2\phi_n\cos^2\theta_n+\cos^2\phi_n)+2D_\parallel t\sin^2\theta_n\sin^2\phi_n \tag{11b}$$

$$\langle\Delta z^2\rangle=2D_\perp t\sin^2\theta_n+2D_\parallel t\cos^2\theta_n\ . \tag{11c}$$

Introducing a "jump" probability $W_i$ for a jump to the adjacent site in the $i$th direction of our lattice, we can write

$$\langle\Delta x_i^2\rangle=2W_i a^2\frac{t}{\tau}\ , \tag{12}$$

where $i=x,y,z$, $\tau$ is the average "lifetime" at each lattice "site," and $a$ is our lattice constant.

Comparing Eqs. (11) and (12) one finds

$$W_x=\frac{D_\perp\tau}{a^2}(1-\cos^2\phi_n\sin^2\theta_n)+\frac{D_\parallel\tau}{a^2}\sin^2\theta_n\cos^2\phi_n\ , \tag{13a}$$

$$W_y=\frac{D_\perp\tau}{a^2}(1-\sin^2\phi_n\sin^2\theta_n)+\frac{D_\parallel\tau}{a^2}\sin^2\theta_n\sin^2\phi_n\ , \tag{13b}$$

$$W_z=\frac{D_\perp-D_\parallel}{a^2}\tau\sin^2\theta_n+\frac{D_\parallel\tau}{a^2}\ . \tag{13c}$$

We can now write

$$G_q(t=p\tau)=\frac{1}{N}\sum_{i=1}^{N}\sum_{\alpha_1}\cdots\sum_{\alpha_p}e^{i\omega_q(\mathbf{r}_i)\tau}W(\mathbf{r}_i,\mathbf{r}_i+\Delta\mathbf{r}_{\alpha_1})e^{i\omega_q(\mathbf{r}_i+\Delta\mathbf{r}_{\alpha_1})\tau}\cdots \times\cdots W(\mathbf{r}_i+\Delta\mathbf{r}_{\alpha_1}+\cdots+\Delta\mathbf{r}_{\alpha_{p-1}},\mathbf{r}_i+\Delta\mathbf{r}_{\alpha_1}+\cdots+\Delta\mathbf{r}_{\alpha_p})e^{i\omega_q(\mathbf{r}_i+\cdots+\Delta\mathbf{r}_{\alpha_p})\tau}\ . \tag{14}$$

Here $N$ is the number of lattice points and $\alpha_j$ is for each $j$ $(j=1,\ldots,p)$ running from 1 to 6 counting all neighboring positions. Jump probabilities $W$ are dependent on the position in the droplet $\mathbf{r}_i+\Delta\mathbf{r}_{\alpha_1}+\cdots+\Delta\mathbf{r}_{\alpha_{p-1}}$ and on the direction of the $p$th jump $\Delta\mathbf{r}_{\alpha_p}$ [Eq. (13)].

Due to the symmetry of the nematic structure, we have $\theta_n(\theta>\pi/2)=\pi-\theta_n(\pi-\theta)$ and since $\omega_q(\theta>\pi/2)=\omega_q(\pi-\theta)$ we can limit our treatment of the self-diffusion to an octant of a droplet. For the fictitious boundaries which separate the chosen octant from the

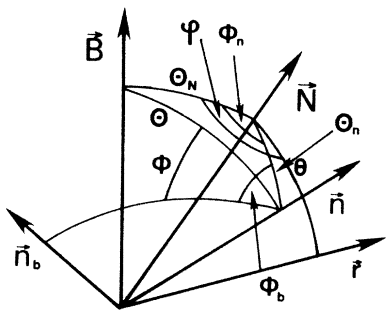


FIG. 3. Schematic illustration of the geometry and angles used in the text. The external field **B** is pointing in an arbitrary direction. The molecular position vector is **r**, **n** is the local director, $\mathbf{n}_b$ the second principal axis of the EFGT, and **N** is the droplet director.

rest of the droplets, we assume reflecting boundary conditions.

$G_q$ is calculated by a simulation of this jump process on a computer, and the line shape is obtained by Fourier transformation. The use of the alternative method based on the inversion matrix[14] is limited by the size of the matrices.

Two-dimensional (2D) deuterium NMR has recently been used to investigate molecular dynamics in the solid state.[15] Although this technique is of difficult application in our case, due to the low intensity of the signals typical of our materials, it has the advantage of providing information independently from fitting procedures based on assumed models and in some cases it could constitute a good probe to study liquid-crystal dynamics in polymer dispersed liquid crystals (PDLC's). In our case, though, both the droplets and the director configurations are more than "assumed models," having been experimentally observed by microscopy techniques in similar samples, and the conventional 1D NMR can provide all the necessary information on molecular diffusion.

We now address some special cases where the dependence of the motional averaging on the bulk value of the quadrupolar splitting $\delta\nu_B$, droplet radius $R$ and average diffusion constant $\bar{D}$ can be easily taken into account.

### A. Slow diffusion

Conditions for the slow-diffusion regime are satisfied when the typical time required for a molecule to diffuse across a distance large enough that the molecular orientation changes appreciably is long compared to $\delta\nu_B^{-1}$. This situation can be achieved in large droplets where $\delta\nu_B R^2/6\bar{D} \gg 1$. In such a case the contribution of the defects, where the motional averaging is absent only for $\bar{D} \to 0$, can be neglected as well. $G_q(t)$ is now given by

$$G_q(t)=\frac{1}{N}\sum_{i=1}^{N} e^{i\omega_q(\mathbf{r}_i)t} \tag{15}$$

and the spectrum by

$$I(\omega)=\frac{1}{N}\sum_{i=1}^{N}\delta[\omega-\omega_q(\mathbf{r}_i)] \; . \tag{16}$$

$I(\omega)$ directly reflects the distribution of $\theta_n$ in the droplet. For example, in the hypothetical case of a radial alignment with constant degree of nematic order and no external field, we get a powder pattern, as all orientations are equally probable.

### B. Fast diffusion

The fast-diffusion regime is defined by $\delta\nu_B R^2/6\bar{D} \ll 1$. This case is much easier to achieve than the slow-diffusion one. From Eq. (6) we have

$$G_q(t)=1+i\int_0^t\langle\omega_q(t')\rangle dt' - \tfrac{1}{2}\int_0^t\int_0^t\langle\omega_q(t')\omega_q(t'')\rangle dt'\,dt''+\cdots \; . \tag{17}$$

In the fast-diffusion regime correlations can be neglected, i.e.,

$$\langle\omega_q(t')\omega_q(t'')\rangle=\langle\omega_q(t')\rangle\langle\omega_q(t'')\rangle \; . \tag{18}$$

The same kind of simplification holds for the higher-order terms and Eq. (6) becomes

$$G_q(t)=\exp\left[i\int_0^t\langle\omega_q(t')\rangle dt'\right] \; . \tag{19}$$

The line shape is then given by

$$I(\omega)=\delta(\omega-\langle\omega_q\rangle) \; . \tag{20}$$

The average quadrupolar shift $\langle\omega_q\rangle$ indirectly reflects the distribution of $\theta_n$. In the spherical droplet with normal molecular alignment on the surface and no applied field, $\langle\omega_q\rangle=0$.

### C. Magnetic field parallel to *N*

In this case ($\theta_N=0$) the frequency $\omega_q$ depends only on the angle $\theta_n$ between **n** and **N** and the angle $\phi_b$,

$$\omega_q=\pm\pi\delta\nu\tfrac{1}{2}(3\cos^2\theta_n-1+\eta\sin^2\theta_n\cos 2\phi_b) \; . \tag{21}$$

Using Eq. (21) in numerical calculation of $G_q(t)$ we can get, after a Fourier transformation, the line shape.

## IV. SAMPLE PREPARATION

The two selectively deuterated liquid-crystal compounds used were 4'-methoxy-4-cyanobiphenyl (10CB) deuterated on the methyl position and 4'-pentoxy-4-cyanobiphenyl (50CB) deuterated on the $\alpha$ position of the alkoxy chain.

Both compounds were prepared by alkylating 4-hydroxy-4'-cyanobiphenyl (EM Laboratories, New York) with the appropriately deuterated halide using the anhydrous method in DMF-benzene previously described for preparing 4-*n*-heptyloxybenzoic acid methyl esters.[16] Perdeuterated methyl iodide was purchased from ICN and 1-bromopentane-1,1-$d_2$ was prepared from the alcohol (obtained by lithium aluminum deuteride reduction of pentanoyl chloride) by treatment with $PBr_3$. Transition temperatures for 10CB were 104.3–104.4 °C for the crystal-to-isotropic transition ($C \to I$), 86.2 °C for

the isotropic-to-nematic transition ($I \rightarrow N$), and 61.2 °C ($N \rightarrow C$), and for 50CB, 47.3–47.7 °C ($C \rightarrow N$), 66.1–66.3 °C ($N \leftrightarrow I$), and 28.0 °C ($N \rightarrow C$). More information will be provided in a later paper.

The dynamics of phase-separation processes involving polymers has been observed and discussed by a number of authors.[17–20] Several methods to obtain phase separation in different mixtures have been used and described.[1,21]

For the NMR experiments described in this paper we used samples prepared using two methods: phase separation by polymerization and phase separation by thermal gelation of a solution exhibiting an immiscibility gap. In the first case, we start with a homogeneous solution of liquid crystal and "prepolymer," two substances that undergo a polymerization reaction. As the reaction proceeds, the average molecular weight of the polymeric molecules increases and the miscibility of the liquid crystal, which at the beginning is complete, is progressively reduced. Droplets of a liquid-crystal-rich phase start to nucleate, surrounded by a polymer-rich phase. The droplet growth continues until gelation of the polymer into a solid freezes in the droplet sizes. The reaction can still proceed due to the residual mobility of the polymer chains and diffusion of the monomers through the liquid-crystal-rich phase. In most cases, the final material contains fairly pure liquid-crystal droplets. When compared to the bulk, the *N-I* transition is broader but typically shifted by only 2 or 3 °C. Rough estimates from scanning electron microscope (SEM) pictures show that a consistent percentage of the initial quantity of liquid crystal is dissolved in the solid matrix, the amount depending mainly on the curing temperature.

Using this technique the size of droplets can be controlled by changing the relative amount of liquid crystal mixed with the prepolymer and/or the temperature of curing. The effect of changing the concentration of liquid crystal is relatively straightforward: below a certain limit, which increases with increasing temperature of curing, no droplets of observable size are formed. Above this limit an increase in concentration causes the droplets to become larger until, for very high concentrations, they become interconnected and channels of liquid crystals are formed in the polymer.

The main effect of a change in the curing temperature is the shift to higher residual concentrations of the liquid crystal in the polymer. In general, a higher temperature of curing gives smaller droplets.

Another method for the preparation of a dispersion of liquid-crystal droplets makes use of thermoplastic polymers where there is little or no crosslinking between chains. One of the macroscopic consequences of this property is that these polymers can melt at relatively low temperatures without any decomposition. By mixing a liquid crystal with one of such substances in the liquid state and then cooling the homogeneous solution, we may eventually enter a region of the phase diagram where the liquid crystal and the polymer are no more completely miscible. So a phase separation starts and proceeds until the polymer becomes a solid. This fixes the droplet size. With fast cooling, the polymer becomes solid long before the thermodynamic equilibrium is reached, droplets do not have time to grow, and their final size is smaller but their number is larger because they do not have time to coalesce. Figure 4 shows this effect in an epoxy-type thermoplastic polymer. SEM observations show that the droplet diameters are never extremely uniform, especially for larger droplets. This feature can influence the line shape in some cases. Figure 5 shows an SEM picture of a section of a surface obtained by cutting the sample which was prepared by a phase-separation process described in this section. The liquid crystal was removed from the opened droplets on the surface by evaporation under a vacuum in order to obtain the SEM pictures.

The materials used for the preparation of the different

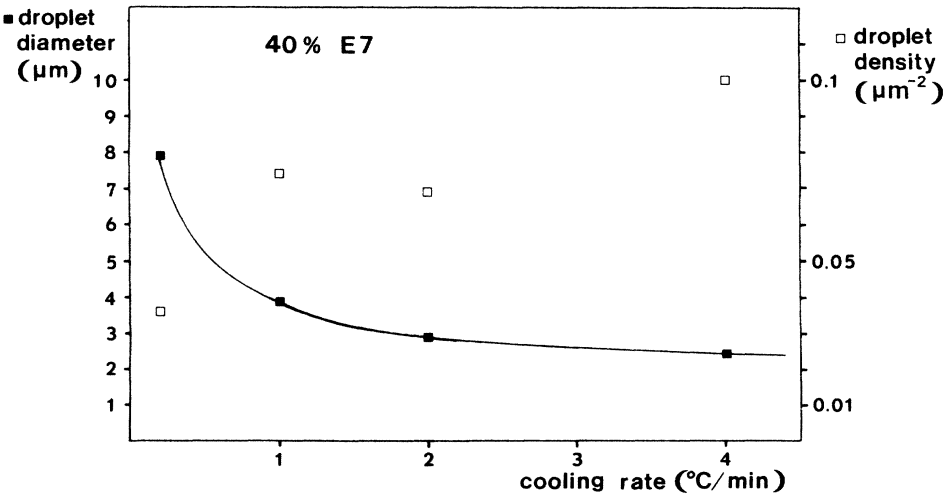


FIG. 4. Average droplet size vs cooling rate using thermoplastic polymer. The liquid crystal is E7 and the polymer was obtained by mixing equal amounts of Epon 828 and *t*-butylamine. The wt. ratio of liquid crystal to polymer was 2:3. The droplet density is defined as the number of droplets counted per unit surface area of a section cut through the sample.

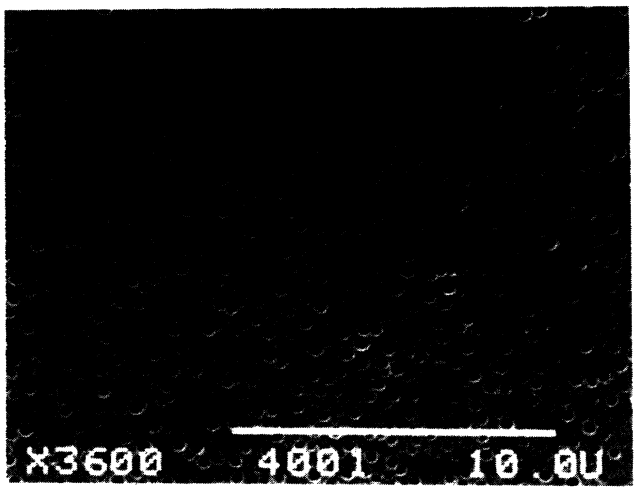


FIG. 5. SEM picture of a cut-through sample of 10CB-$d_3$/E20 in an epoxy resin (Bostik), used for NMR experiments described in this paper. The liquid crystal was removed from the open droplets and the polymer matrix is shown in the figure.

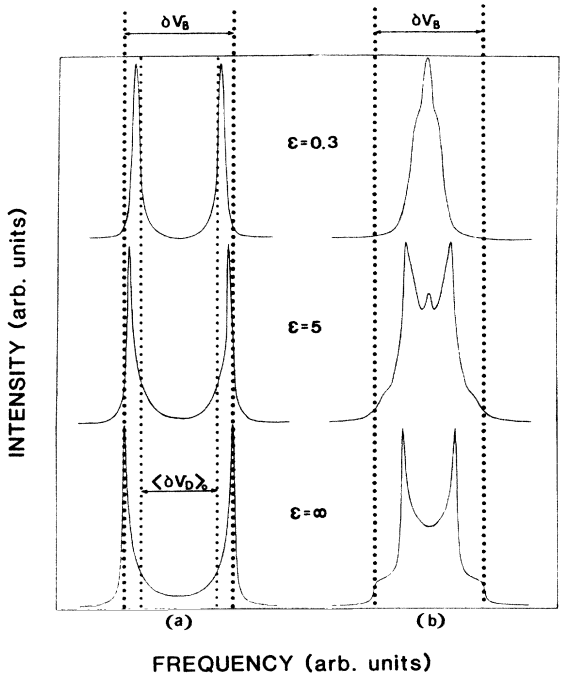


FIG. 6. Simulated spectra for droplets with their symmetry axes in the direction of a weak ($R/\xi=0.5$) magnetic field for bipolar (a), and star (b) director configurations. $\delta\nu_B$ is the bulk splitting and $\langle\delta\nu_D\rangle_0$ is the splitting in the case of a very fast diffusion ($\epsilon\simeq 0$), when the frequency is averaged over all director orientations in the droplet.

samples were obtained from BDH Chemicals, England (E7, E20), Shell Chemical Co., Houston, TX (Epon 828), Kodak, Rochester, NY (*s*-butylamine, *t*-butylamine), and Bostik SpA, Italy (Bostik).

## V. EXPERIMENTS AND COMPARISON WITH THEORY

As previously mentioned, the electric field gradient tensor at a nuclear site can be additionally averaged by translational diffusion in nematic droplets. The effectiveness of diffusional averaging in a droplet with radius $R$ is characterized by the parameter

$$\epsilon=\frac{\delta\nu_B R^2}{12\bar{D}}\ , \tag{22}$$

where $\delta\nu_B$ is the bulk nematic phase DMR splitting, and $\bar{D}$ the average diffusion coefficient. Theoretical line shapes from droplets in a weak field, $R/\xi=0.5$, obtained using the previously described jump model for the anisotropic diffusion ($D_\parallel/D_\perp=2$) are shown in Fig. 6 for different values of the parameter $\epsilon$ and for tangential and normal alignment on the surface. No biaxiality is taken into account ($\eta=0$). It is evident that the change in the line shape corresponding to a variation of $\epsilon$ is much more significant in the case of a "star" configuration with normal anchoring than in the bipolar configuration. In the bipolar case the line shape does not change much, other than for the apparent line-splitting reduction from the bulk value $\delta\nu_B$ for $\epsilon\gg 1$ to $\langle\delta\nu_D\rangle_0$, which is the splitting in the fast-diffusion limit where $\epsilon=0$. It is worthwhile to stress that for $\epsilon=\infty$ the apparent lines are edge singularities of a distribution, while in the limit $\epsilon=0$ they are real lines, due to the averaging effect of molecular diffusion through all different positions of the distribution.

Figure 7(a) shows a DMR spectrum obtained from nematic droplets dispersed in a thermoplastic polymer. The liquid crystal used in 10CB, deuterated on the methyl group and mixed in a ratio of 1:2 with British Drug House E20. The mixture was used to facilitate sample preparation. The polymer is a result of a reaction of the epoxy resin Epon 828 with *s*-butylamine in a ratio 1:1 in equivalent weights. The polymer–liquid-crystal mixture was cooled from the homogeneous liquid phase at $\sim$200 °C to room temperature in a magnetic field of 4.7 T at a rate of 0.3 °C/min. With this cooling rate, we were able to obtain relatively large droplets with a radius $R\simeq 3.5$ $\mu$m so that their symmetry axes were uniformly oriented in the direction of the magnetic field. The line shape obtained from this sample [Fig. 7(a)] agrees quite well with the simulated one for $\epsilon=\infty$ and bipolar director configuration [Fig. 7(b)]. The bulk spectrum [Fig. 7(c)] is shown for comparison.

The nematic splitting from the $\alpha$ position in 50CB is about ten times larger than that of the methyl group on 10CB and the averaging effect of diffusion is very different in the two cases. Figure 8 shows the molecular structure of these two compounds and presents the measured effective nematic splitting in the bulk and in the relatively small droplets ($R/\xi<0.3$) together with their ratio. The values of the orientational order parameter $S$ in the bulk case and the effective $\langle S\rangle$ in the droplet case are calculated using the well-known formula

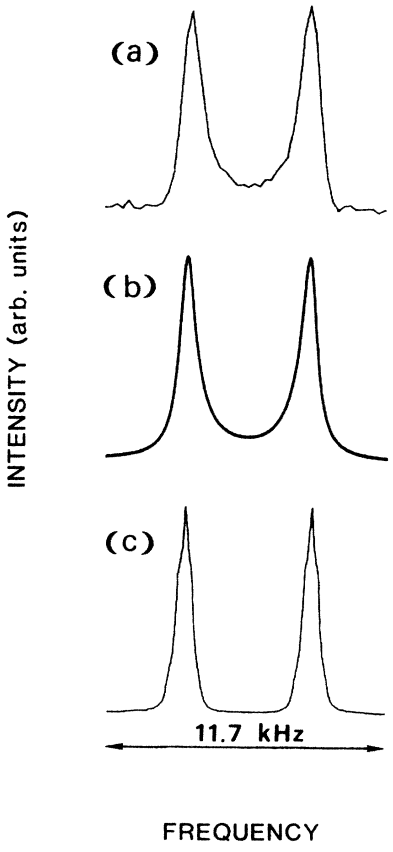


FIG. 7. Spectrum obtained at 27°C from large nematic droplets of the 10CB/E20 mixture with $\epsilon > 50$ (a), compared to the simulated line shape for a bipolar configuration in aligned droplets with $\epsilon = \infty$ (b). The bulk spectrum (c) at the same temperature is also shown.

$$\begin{bmatrix} \delta\nu_B \\ \langle \delta\nu_D \rangle \end{bmatrix} = \frac{3}{2}\frac{(3\cos^2\theta_0 - 1)}{2}\nu_Q \begin{bmatrix} S \\ \langle S \rangle \end{bmatrix}, \tag{23}$$

where $\nu_Q$ is the solid-state quadrupolar coupling constant, $\sim 175$ kHz for a deuterium atom on an $sp^3$ carbon atoms,[22] $\delta\nu_B$ and $\langle \delta\nu_D \rangle$ are the measured splittings, and $\theta_0$ is, for instance, the carbon-oxygen-carbon angle in the case of 10CB.[23] The principal axis of the order matrix was assumed to coincide with the molecular long axis and the additional averaging due to fast rotation along the O—$CD_3$ bond in the 10CB was taken into account. In these relatively small droplets, $R/\xi < 0.3$, the diffusion-induced narrowing is quite pronounced for 10CB-$d_3$, $\epsilon \simeq 0.2$. The low values of the ratio $\langle \delta\nu_D \rangle / \delta\nu_B \sim 0.7$–$0.8$ agree quite well with the calculated diffusion narrowing for a bipolar structure with $R/\xi \sim 0.3$ and $\epsilon = 0$ (see Fig. 9). In the case of 50CB-$\alpha d_2$ the droplets are approximately the same size but the value of $\epsilon$ is much larger, mainly due to the larger splitting, and the value of $\langle \delta\nu_D \rangle / \delta\nu_B$ is approximately 0.9.

As far as the temperature dependence of this ratio is concerned, its variation is too small, compared to the error, to allow final conclusions. Nevertheless, we can infer some information. Near the transition we expect an increased field-induced ordering ($R/\xi \propto S^{-1/2}$) and therefore an increase in $\langle \delta\nu_D \rangle / \delta\nu_B$. This is evident in the 10CB data, where because of the diffusion narrowing ($\epsilon \sim 0.2$) a change in configuration is reflected in an increase of the spectrum width $\langle \delta\nu_D \rangle$. For 50CB ($\epsilon \sim 4$) the same change in configuration causes more a redistribution in spectral intensity rather than narrowing. In this case, the only noticeable effect is an increase of the ratio at lower temperatures, as it is observed in both 10CB and 50CB data, probably due to an increase in $\epsilon$

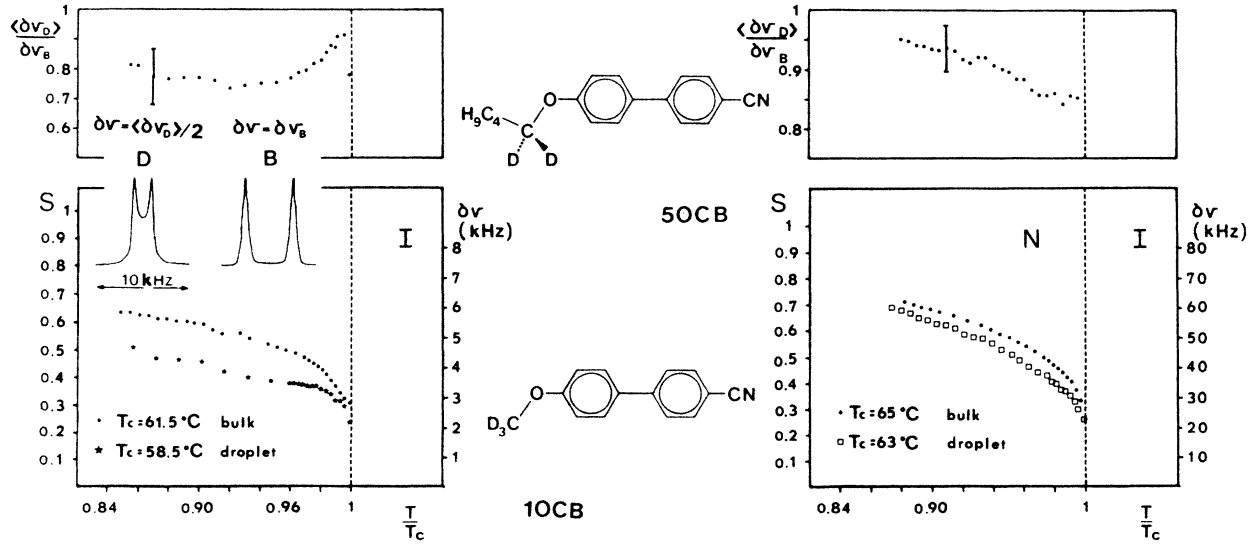


FIG. 8. Nematic splittings for the bulk ($B$) and the droplets ($D$) of 10CB-$d_3$/E20, 50CB-$\alpha d_2$, and their ratio. The effective orientational order parameter is presented as well. The polymer used was the epoxy resin Bostik with parts $A$ and $B$ in the ratio 1:1. The ratio of liquid crystal to polymer was 1:2. The molecular structure of the deuterated compounds and the line shapes for 10CB-$d_3$ in droplets and in the bulk nematic at 36°C are shown as insets.

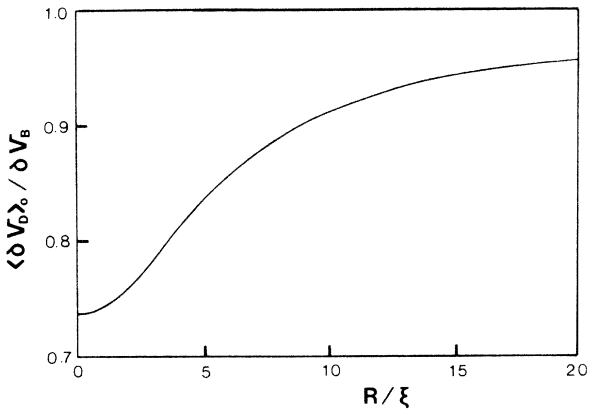


FIG. 9. Diffusion-reduced splitting calculated for a bipolar structure in the fast-diffusion limit ($\epsilon=0$) as a function of the external field strength. The bulk nematic splitting is $\delta\nu_B$ and the droplet splitting for $\epsilon=0$ is $\langle\delta\nu_D\rangle_0$.

through the temperature dependence in $\nu_B$ and $\bar{D}$.

A typical spectrum from 10CB-$d_3$ in droplets for which $R/\xi\sim 0.3$ is shown as an insert in Fig. 8. It is powderlike with two singularities separated by $\frac{1}{2}\langle\delta\nu_D\rangle$. These indicate a random distribution of the droplet directors even in the presence of the magnetic field. Such a situation occurs in small droplets where the effect of the magnetic field cannot overcome the effect of the surface.

When the process of droplet formation is occurring in an external field, an interesting effect of field-induced, frozen-in partial droplet alignment can be detected by DMR. By cooling a homogeneous liquid mixture of a thermoplastic polymer and a liquid crystal rapidly in the presence of a magnetic field, we were able to obtain a material which gave the DMR spectra shown in Fig. 10. During the acquisition of the spectrum in Fig. 10(a) the external field was in the same direction as during the cooling process, while the spectrum in Fig. 10(b) was taken after a rotation of the sample by 90° around a direction normal to the field. It is clear from these spectra that there is a preferential molecular orientation along the direction of preparation. When the sample is cooled without the presence of an external field a random distribution of droplet directors is frozen in and the DMR spectrum is powderlike for all directions of $B$.

Another way to achieve the partial droplet-director orientation is to cure a sample in the presence of an external field in which droplets are formed through phase separation induced by polymerization. The effect is present if the isotropic-nematic transition in the droplets occurs before the gelation of the surrounding polymer. Figure 11 shows spectra obtained from droplets of 10CB-$d_3$/E20 in an epoxy-type polymer cured in the

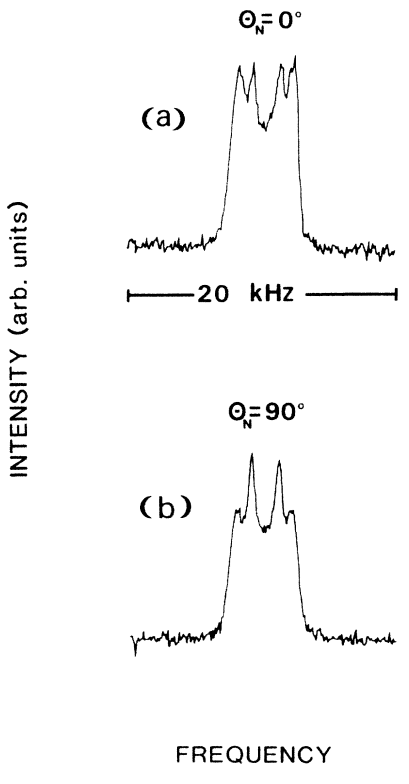


FIG. 10. Spectra from droplets of 10CB-$d_3$/E20 in a thermoplastic polymer (Epon 828/$s$-butylamine) after rapid cooling through the glass transition in the presence of a 4.7-T external field. The angle between the external field **B** and the "curing direction" is $\theta_N$, the temperature is 36 °C.

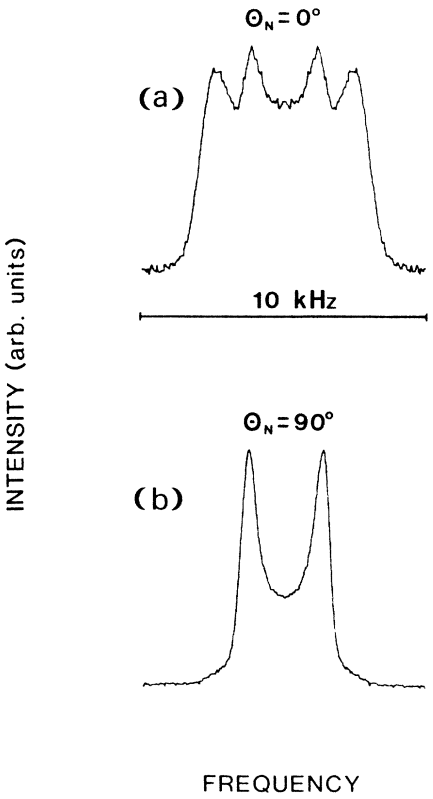


FIG. 11. Spectra from droplets of 10CB-$d_3$/E20 in the epoxy resin Bostik cured in the presence of a 4.7-T magnetic field. The angle $\theta_N$ is measured between the external field **B** and the curing direction, the temperature is 5 °C.

presence of a 4.7-T magnetic field. For the spectrum in 11(a), the static field was along the curing direction, while for the spectrum in 11(b) the angle between the external field and the curing direction was 90°. We can clearly see that the frozen orientation of droplet directors cannot be destroyed by a magnetic field of 4.7 T. The frozen molecular alignment is a permanent characteristic of these materials. Samples tested after two years from their preparation showed only a slight decrease in the degree of induced orientation, as observed from DMR spectra. The droplet-director alignment is also clearly detectable from the light polarizing properties of thin films of these materials.

The origin of the freezing in of a certain director ordering is not clear yet and at least two different explanations are possible. The presence of the nematic phase at the droplet interface during its formation can induce an anisotropic polymer chain growth and orientation which, in turn, will affect the liquid-crystal orientation at the droplet walls when the curing process is completed. Also, a bipolar nematic droplet in a liquid medium has a prolate spheroid equilibrium shape. Therefore, droplets which are already in the nematic phase before gelation occurs will be permanently elongated. If there is no external field there is no preferred orientation of the droplet director and a random distribution is frozen in. The presence of the external field while the surrounding of the droplets is still soft results in a partial ordering of the droplet directors which is then frozen in by the gelation.

To investigate the possibility of the droplet-director orientation by nonspherical droplets, DMR spectra were taken of samples subjected to mechanical stress. Figure 12 shows two of these spectra in which the compression on the sample was in a direction normal [12(a)] and parallel [12(b)] to external field. In this case the expected shape of the droplet is approximately an oblate spheroid with the short axis in the direction of the stress. In such a droplet, its director prefers to be in the plane orthogonal to the short axis, which means that by such stress we can partially induce a planar type of ordering. As expected the spectrums in 12(a) and 12(b) show the effect of a partial planar-type ordering.

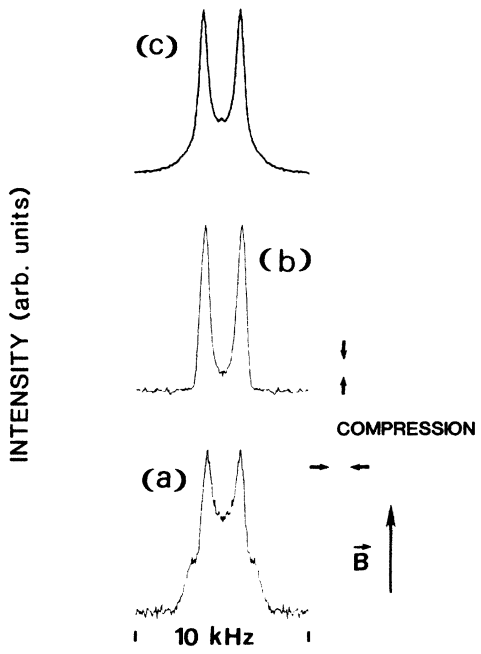


FIG. 12. Spectra from droplets of 10CB-$d_3$/E20 in the epoxy resin Bostik at 25 °C. The sample is compressed along a direction normal (a) and parallel (b) to the external magnetic field. A spectrum from a sample of the same material not subjected to stress at the same temperature (c) is also shown.

## VI. CONCLUSIONS

We have shown how DMR can be used to monitor the director configuration in nematic microdroplets. A theoretical model is presented to simulate line shapes taking into account translational diffusion-induced narrowing and the results have been compared to experimental spectra. NMR line shape is shown to be sensitive to the type of the director configuration, quadrupole splittings, diffusion constants, external field, droplet size, and shape. We have also observed how the presence of an external field during droplet-formation process can be memorized by the freezing of the droplet-director alignment and we have shown how the effect of mechanical stress on a droplet structure can be observed via DMR.

## ACKNOWLEDGMENTS

The authors wish to acknowledge Katherine Leung and Micheal Jirousek for their synthesis work, Maja Žumer for her computer calculations. The research was supported in part by the National Science Foundation under (Solid State Chemistry Program) Grants No. DMR-85-15221, and No. DMR-85-03219.

*Permanent address: Department of Physics, E. Kardelj University of Ljubljana, Jadranska 19, YU-61000 Ljubljana, Yugoslavia.

[1]J. W. Doane, N. A. Vaz, B.-G. Wu, and S. Žumer, Appl. Phys. Lett. **48**, 4 (1986).

[2]J. Fergason, SID Int. Symp. Digest Tech. Papers **16**, 68 (1985).

[3]E. Dubois-Vilette and O. Parodi, J. Phys. (Paris) Colloq. **C4**, 57 (1969).

[4]S. Candau, P. LeRoy, and F. Debeauvais, Mol. Cryst. Liq.

Cryst. **23**, 283 (1973).
[5]G. E. Volovik and O. D. Lavrentovich, Zh. Eksp. Teor. Fiz. **85**, 1997 (1983) [Sov. Phys.—JETP **58**, 1159 (1983).
[6]S. Žumer and J. W. Doane, Phys. Rev. A **34**, 3373 (1986).
[7]P. G. de Gennes, *The Physics of Liquid Crystals* (Clarendon, Oxford, 1974).
[8]S. Žumer and J. W. Allender, Bull. Am. Phys. Soc. **31**, 691 (1986).
[9]M. J. Press and A. S. Arrot, Phys. Rev. Lett. **33**, 403 (1974).
[10]R. D. Williams, Rutherford Appleton Laboratory Report No. RAL 85-062, 1985 (unpublished).
[11]P. S. Drzaic, (private communication).
[12]D. W. Allender, G. L. Henderson, and D. L. Johnson, Phys. Rev. A **24**, 1086 (1981).
[13]W. F. Ames, *Numerical Methods for Partial Differential Equations* (Academic, New York, 1977).
[14]A. Abragam, *The Principles of Nuclear Magnetism* (Oxford University Press, London, 1961).
[15]C. Schmidt, S. Wefing, B. Blümich, and H. W. Spiess, Chem. Phys. Lett. **130**, 84 (1986).
[16]M. E. Neubert, S. J. Laskos, Jr., L. J. Mauer, L. T. Carlino, and J. P. Ferrato, Mol. Cryst. Liq. Cryst. **44**, 197 (1978).
[17]J. W. Cahn, J. Chem. Phys. **42**, 93 (1965).
[18]O. Olabisi, L. M. Robeson, and M. T. Shaw, *Polymer-Polymer Miscibility* (Academic, New York, 1979).
[19]M. Kurata, *Thermodynamics of Polymer Solutions* (Harwood Academic, Switzerland, 1982).
[20]H. Strathmann, in *Material Science of Synthetic Membranes,* edited by D. R. Lloyd (American Chemical Society, Washington, D.C., 1985).
[21]B.-G. Wu, J. L. West, and J. W. Doane, J. Appl. Phys. (to be published).
[22]L. J. Burnett and B. H. Muller, J. Chem. Phys. **55**, 5829 (1971).
[23]H. M. Seip and M. Seip, Acta Chem. Scand. **27**, 4024 (1973).

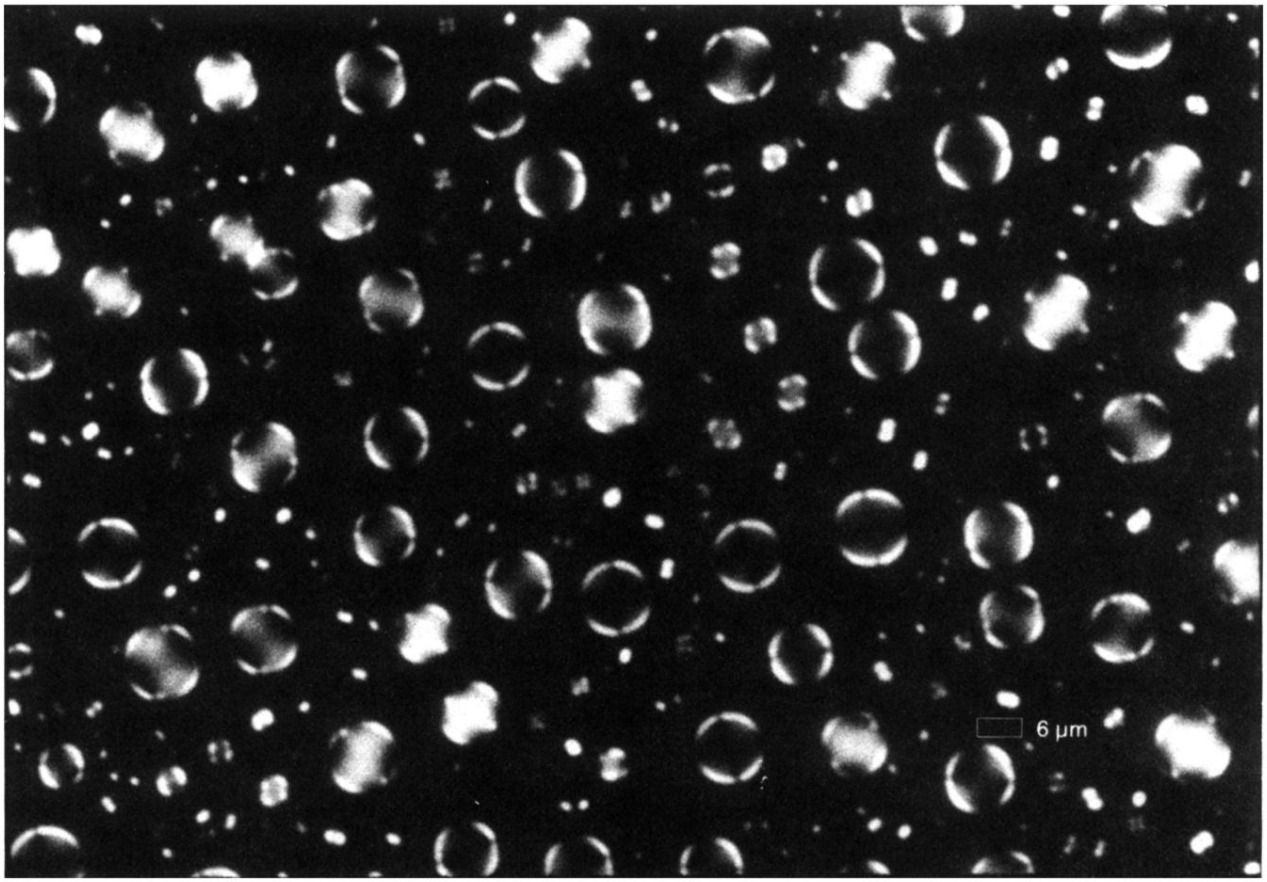


FIG. 2. Optical microscope picture of droplets of British Drug House E7 dispersed in an epoxy resin obtained by mixing equal amounts of Epon 828 and *t*-butylamine. The sample is positioned between crossed polarizers.

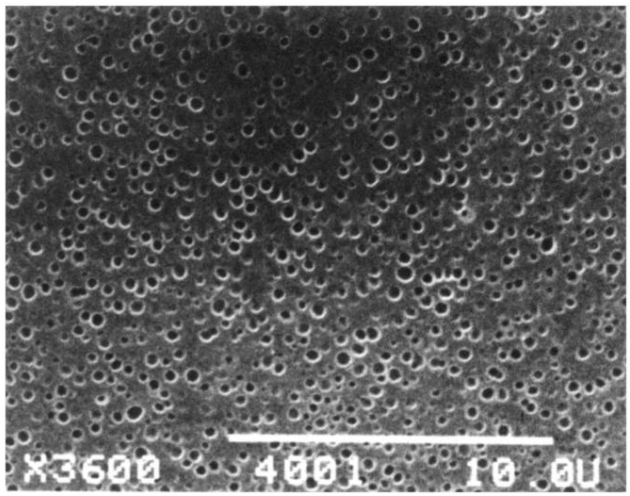


FIG. 5. SEM picture of a cut-through sample of 10CB-$d_3$/E20 in an epoxy resin (Bostik), used for NMR experiments described in this paper. The liquid crystal was removed from the open droplets and the polymer matrix is shown in the figure.